01 Jan 1974

Measurements Of The Average Electric Dipole Polarizabilities Of The Alkali Dimers

Robert W. Molof

Thomas M. Miller

Henry L. Schwartz

Benjamin Bederson

et. al. For a complete list of authors, see https://scholarsmine.mst.edu/phys_facwork/2387

Recommended Citation

R. W. Molof et al., "Measurements Of The Average Electric Dipole Polarizabilities Of The Alkali Dimers," *The Journal of Chemical Physics*, vol. 61, no. 5, pp. 1816 - 1822, American Institute of Physics, Jan 1974. The definitive version is available at https://doi.org/10.1063/1.1682180

RESEARCH ARTICLE | AUGUST 22 2003

Measurements of the average electric dipole polarizabilities of the alkali dimers

Robert W. Molof; Thomas M. Miller; Henry L. Schwartz; Benjamin Bederson; John T. Park

J. Chem. Phys. 61, 1816–1822 (1974)
https://doi.org/10.1063/1.1682180

Measurements of the average electric dipole polarizabilities of the alkali dimers*

Robert W. Molof, Thomas M. Miller, Henry L. Schwartz, Benjamin Bederson, and John T. Park†

Physics Department, New York University, New York, New York 10003
(Received 2 May 1974)

The average electric dipole polarizabilities of the homonuclear alkali dimers have been measured in an electric deflection experiment. The molecular results are normalized to the corresponding atomic polarizabilities by comparing deflections of atomic and molecular alkali beams passing through an inhomogenous electrostatic field. The average polarizabilities in units of 10^{-24} cm^3 are: Li_2(990°K), 34 ± 3; Na_2(736°K), 30 ± 3; K_2(569°K), 61 ± 5; Rb_2(534°K), 68 ± 7; Cs_2(515°K), 91 ± 7.

I. INTRODUCTION

The dc electric dipole polarizability is a tensor property of the molecular charge distribution which appears in the description of a number of physical phenomena such as Rayleigh and Raman scattering, optical dispersion, the Kerr effect, van der Waals attraction, and low-energy charged-particle scattering from neutral molecules. The polarizabilities of the diatomic alkali molecules have not been measured previously and to our knowledge only one published calculation exists,[1] treating the polarizability of Li_2. The alkali dimers have been studied in optical experiments[2] for many years and recently have been used in scattering experiments in collisions with atoms[3] and with electrons.[4]

In the present experiment, we have used an electric deflection technique to measure the average values of the static electric dipole polarizabilities of the homonuclear alkali dimers, relative to the corresponding atomic polarizabilities. The scalar polarizabilities of the alkali metal atoms are known to within 2% from a separate experiment utilizing a different technique but performed on this same apparatus.[5] For each of the alkali dimers, we measure a polarizability value which is an average of the tensor components of the polarizability and is an average over the rotational and vibrational distributions characteristic of the temperature of our beam source. Furthermore, the measurement takes place in a magnetic field that decouples the nuclear and rotational angular momenta. The measured quantity will be explicitly discussed in Sec. II.

II. THEORY

In the presence of an electric field $\mathbf{E}$, a dipole moment is induced in the alkali atoms or molecules. The induced dipole moment $\mathbf{p}$ of the system can be expanded in powers of the applied electric field. For the homonuclear molecules, there is no second order term, and terms of higher order in the electric field, while important for nonlinear effects (e.g., scattering of intense laser beams) can be ignored for the relatively small fields of the present experiment. Thus, we are concerned only with the term

$$\mathbf{p} = \alpha \cdot \mathbf{E} , \tag{1}$$

which defines the tensor polarizability α. The corresponding change ΔU in the energy is given to second order by

$$(\Delta U)_2 = -\tfrac{1}{2}\mathbf{E} \cdot \alpha \cdot \mathbf{E} . \tag{2}$$

If $\mathbf{E}$ is small compared to the atomic field, then the energy correction to the unperturbed Hamiltonian is also small and can be treated as a perturbation. Evaluating the second order correction $(\Delta U)_2$ and making use of Eq. (2), one finds the components α_{ij} of the polarizability tensor[6]:

$$\alpha_{ij} = 2\sum_{k\neq 0} \frac{\langle 0|\sum_m e r_{mi}|k\rangle\langle k|\sum_n e r_{nj}|0\rangle}{\mathcal{E}_k - \mathcal{E}_0} , \tag{3}$$

where e is the electronic charge, r_{ab} is the bth position coordinate of the ath electron, $\mathcal{E}_0$ is the unperturbed ground-state energy, and $\mathcal{E}_k$ is the energy of an unperturbed excited state of the system.

For the alkali atoms, which have essentially an isotropic charge distribution in the ground state, the polarizability tensor reduces to a single scalar quantity[6] which we refer to as the polarizability α. For the homonuclear alkali dimers, there is clearly a charge asymmetry. If the z axis is chosen to be along the internuclear axis in a molecule-fixed reference frame (x, y, z), then the polarizability tensor is diagonalized and has only two independent components α_{zz} and α_{xx}, since $\alpha_{xx} = \alpha_{yy}$. However, these values depend on the rotational and vibrational state of the molecule.

It is common to define two alternative quantities to describe the polarizability tensor: the average polarizability $\bar{\alpha}$,

$$\bar{\alpha} = (\alpha_{zz} + 2\alpha_{xx})/3 \tag{4}$$

and the polarizability anisotropy γ,

$$\gamma = \alpha_{zz} - \alpha_{xx} . \tag{5}$$

Variational and semiempirical methods have been used to calculate polarizabilities, but the majority of the calculations performed have used perturbation techniques. Calculations for the alkali atoms are numerous and have been discussed elsewhere.[5,6] Only one published calculation exists for an alkali dimer—that of Kolker and Karplus,[1] who used an uncoupled Hartree–Fock approximation to calculate $\bar{\alpha}$ and γ for Li_2. Unpublished work on Li_2 and Na_2 has been done by Bottcher.[7]

In our experiment, magnetic and electric fields are applied transverse to the directions of the atomic or molecular beam. The magnetic fields used in this experiment were sufficient to decouple the nuclear spin I

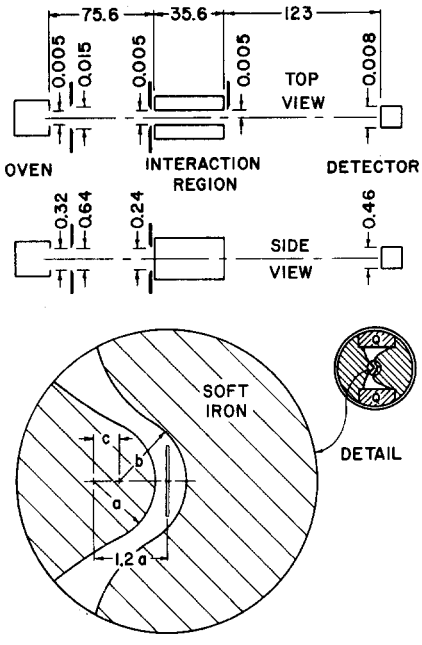

FIG. 1. A diagram of the apparatus giving relevant dimensions in centimeters. At the bottom of the figure is a detail cross section of the pole pieces of the interaction region. Quartz spacers are marked with a Q. The design parameters are $a = 0.159$ cm, $b = 0.172$ cm, and $c = 0.066$ cm.

and the rotational angular momentum J.[8] Thus, J is a good quantum number. Without the magnetic field, the rotational average of the polarizability in the laboratory reference frame is greatly complicated. The problem of a molecule in simultaneous electric and magnetic fields has been analyzed by MacAdam and Ramsey.[9] In our case, the diagonalization of the electric and magnetic parts of the Hamiltonian is simplified because the off-diagonal magnetic terms and the external electric field coupling between states of different J are small.[8] The beam deflection in our experiment depends on $\alpha_{ZZ}(J, m_J)$ for applied fields along the Z direction in a laboratory frame of reference (X, Y, Z), and $\alpha_{ZZ}(J, m_J)$ may be found from the diagonalized Hamiltonian with Eq. (2):

$$\alpha_{ZZ}(J, m_J) = \bar{\alpha}(J) + \frac{\gamma(J)}{3}\left\{3\left[\frac{(J-m_J)(J+m_J)}{(2J+1)(2J-1)} + \frac{(J+m_J+1)(J-m_J+1)}{(2J+1)(2J+3)}\right] - 1\right\} . \quad (6)$$

Our experiment does not distinguish different m_J states, so that the result is an average over m_J values,

$$\frac{1}{2J+1}\sum_{m_J} \alpha_{ZZ}(J, m_J) = \bar{\alpha}(J) . \quad (7)$$

There is also a dependence on the vibrational quantum number v which we have not explicitly shown. The experimentally observed polarizability is an average over the thermal rotational and vibrational state distributions.[10] We will refer to the measured quantity as $\langle\bar{\alpha}\rangle_{J,v}$.

III. APPARATUS

Figure 1 is a schematic diagram of the apparatus giving relevant dimensions. The apparatus consists of a conventional alkali oven as a beam source, an interaction region where inhomogeneous electric and magnetic fields may be applied, and a platinum surface-ionization beam detector. The detector chamber is movable perpendicular to the beam axis (in order to detect the deflected beam), and a dial gauge accurate to about 10^{-4} cm was used to indicate the detector displacement. The oven temperatures used depended on the species studied and are specified in Sec. V, but were typically 500 °K or higher. At the temperatures used, the alkali vapor pressure in the oven was a few hundred millitorr, which was low enough to give an effusive beam and high enough to give a sufficient dimer component (~1%). The background gas pressures in the apparatus were typically 5×10^{-7} torr in the source chamber with a beam operating, and $< 10^{-8}$ torr in the remainder of the apparatus.

In the interaction region, the beam passes between two iron pole pieces which are insulated from each other. The "two-wire" configuration is the same as that described by Salop, Pollack, and Bederson[11] although the size and mounting of the pole pieces are different here. The pole pieces are illustrated in cross section in Fig. 1. The iron pole pieces are part of an electromagnet with yoke and coil external to the vacuum system and are used to apply an inhomogeneous magnetic field across the beam axis. Electrodes attached to the pole pieces allow a congruent inhomogeneous electric field to also be applied across the beam axis. With the configuration used here, it can analytically[11] be shown that the ratio of the field gradient to the field strength is reasonably constant over the height of the beam when the beam passes at the position shown in Fig. 1. The ratio of the field gradient to the electric field strength at the beam axis has been measured to be 6.8 cm^{-1} (Sec. VI). At the beam axis, the magnetic field strength can be made as high as 10 kG and the electric field strength can be made as high as 2×10^5 V/cm. The pole pieces have a beam-defining slit mounted at the entrance and a half-slit mounted at the exit end of the interaction region. The half-slit is mounted on the weak-field side of the interaction region so that it does not interfere with the deflection of the beam.

The detected particle count rate was stored in successive channels of a 400-channel multiscaler while the multiscaler incrementally increased the magnitude of an electric potential applied across the pole pieces.

IV. EXPERIMENTAL METHOD

In this experiment, we compare the deflection of an alkali molecular beam to the deflection of the corresponding alkali atom, in an inhomogeneous electric field. Since the polarizabilities of the alkali atoms are known,[5] the average polarizabilities of the molecules may be obtained from the comparison without the need to determine any apparatus parameters absolutely. The method involves deflections of the beam that are greater than the beam width at the detector and are therefore larger deflections than with either the "small shift" or "large

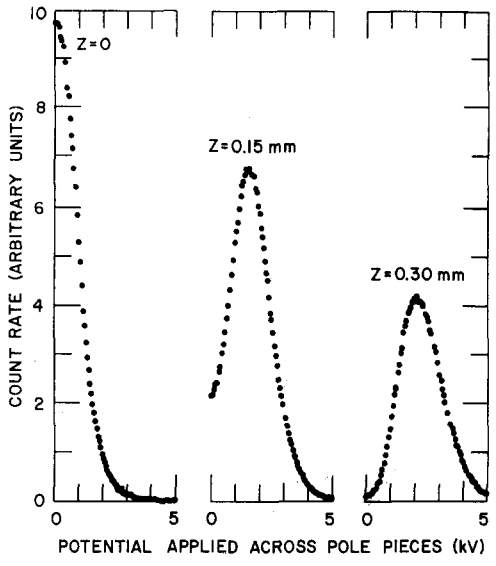

FIG. 2. Electric deflection spectra for rubidium atoms. The detector is positioned off the beam axis by the distance Z given in the figure and the potential across the pole pieces is stepped at 50 V per point, which scans the beam across the detector slit.

shift" techniques previously discussed in the literature.[6] (We deflect, at most, 0.051 cm a beam which is 0.02 cm full width at half-maximum.) An inhomogeneous magnetic field in the interaction region is used to eliminate alkali atoms from the beam in order to observe the molecular beam alone. This is possible because the alkali atoms possess magnetic moments on the order of 1 bohr magneton, while the molecules possess net magnetic moments on the order of a nuclear magneton.

Our procedure is as follows. With a beam operating, we align the pole pieces of the interaction region by scanning the front of the assembly across the beam to maximize the beam intensity at the detector. From the beam intensity patterns obtained by independently scanning the rear of the assembly across the beam, the rear of the interaction region (with half-slit attached) may be positioned. This procedure places the beam along the proper path through the interaction region. Then the detector is scanned across the beam to check the beam profile and center position. Next the detector is moved off axis in order to obtain deflection data. If deflection of an atomic beam is desired, the magnetic field strength in the interaction region is left at zero. If electric deflection of a molecular beam is desired, the magnetic field strength at the beam axis is set to about 2 kG, clearing the beam of atoms. The multiscaler is then set to scan incrementally the potential applied across the pole pieces, with predetermined starting and finishing potentials that will allow adequate resolution of the deflection beam maximum. In operation, the multiscaler accumulates a count rate proportional to the detected intensity for each applied potential value between the starting and finishing potentials. The data acquisition continues, with multiple sweeps, until the signal-to-noise ratio is considered satisfactory—a total time of 0.2–1 h depending on the full beam intensity and on the amount of deflection. Typical spectra are shown in Fig. 2 for rubidium atoms for different deflection distances. Each is a plot of the count rate vs the applied potential (proportional to the electric field strength). The change in potential from point to point in the spectra is 50 V. Normally, we consider only the top half of each spectrum, scanning 1 kV on each side of the maximum. This procedure gives us the potential corresponding to the maximum within 20 V, out of several thousand total. The peak corresponds to a velocity of about $\sqrt{2}$ times the most probable velocity in the oven[8] but is irrelevant insofar as our relative polarizability measurements are concerned. The question as to whether the atomic and molecular velocity distributions may be perturbed by background gas is addressed in Sec. VI, along with a discussion of other possible errors.

Spectra such as those in Fig. 2 were obtained for many detector positions off the beam axis for a given alkali atomic or molecular species, in an overlapping fashion. In most cases, data were obtained at more than one temperature. The temperatures did not differ by more than 5% in these cases, but the changes were such as to significantly affect the atomic and molecular beam intensities both absolutely and relatively. For each spectrum obtained for a particular atom or molecule, the applied potential corresponding to the maximum intensity was determined and a plot of the square of these potential maxima vs detector position was made. Examples are given in Fig. 3 for Rb and Rb_2 at 534 °K. Each point was obtained from the peak of a separate spectrum of the type illustrated in Fig. 2.

It is clear from Fig. 3 that (a) the molecule is deflected considerably more than is the atom for the same applied electric field strengths, (b) the plot of V^2 vs Z yields approximately a straight line, and that (c) the extrapolated straight line does not pass through zero. In the Appendix, an analysis of the experiment is given

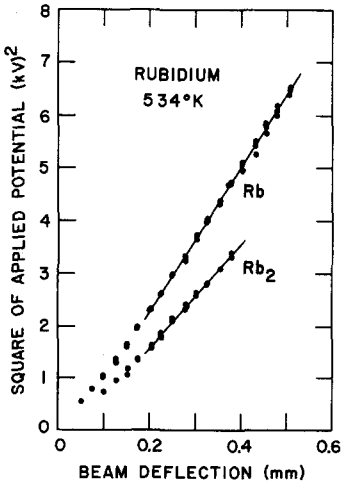

FIG. 3. Typical results obtained from the electric deflection spectra. The square of the potentials corresponding to the maxima of the deflection spectra is plotted vs the detector position off axis. The slope of the resulting line is inversely proportional to the polarizability. For a given applied potential, the molecular beam is deflected considerably more than is the atomic beam.

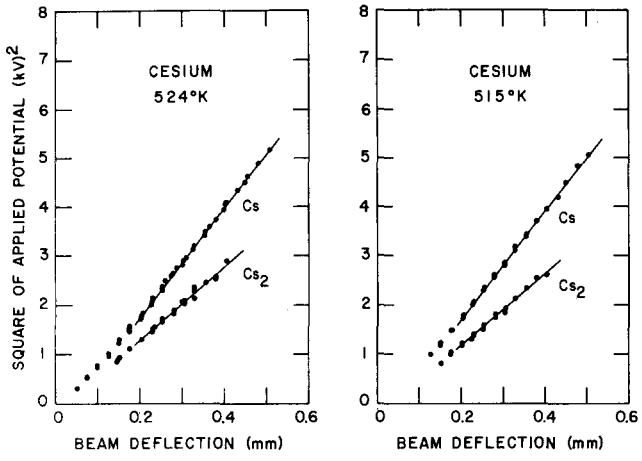

FIG. 4. Electric deflection results obtained for atomic and molecular cesium beams. The slope of the deflection line is proportional to T/α.

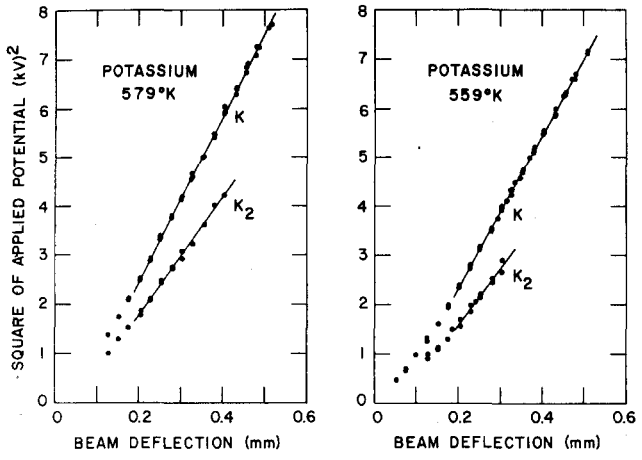

FIG. 6. Electric deflection results obtained for atomic and molecular potassium beams. The slope of the deflection line is proportional to T/α.

which shows that (a) for a beam of infinitesimal width, the plot of V^2 vs Z should be a straight line with a slope inversely proportional to the polarizability of the beam particles; (b) for a beam of finite width, the plot of V^2 vs Z departs from straight-line behavior near the beam axis but asymptotically approaches the infinitesimal beam result for large deflections; and (c) for the molecular beam, the averaging over J, m_J, and v that takes place in our apparatus is equivalent to the desired thermal average of the polarizability $\langle\bar{\alpha}\rangle_{J,v}$. From the analysis in the Appendix, we conclude that the ratio of the atomic and molecular data slopes yields the inverse ratio of the polarizabilities with no correction factors or apparatus parameters involved in the calculation, assuming that relative values of (V, z) for the atomic and molecular data have been correctly measured.

V. RESULTS

Figure 4 shows data obtained for Cs and Cs_2 at 524 and 515 °K. The inverse ratio of the data slopes indicates an average molecular polarizability of 1.51 and 1.54 times the atomic scalar polarizability, respectively. Similar data were obtained[8] for a temperature of 506 °K yielding a ratio of 1.53.

Figure 5 shows data obtained for Rb and Rb_2 at 543 and 524 °K which yield an average molecular polarizability of 1.36 and 1.53 times the atomic scalar polarizability, respectively. Data obtained for 534 °K yield a ratio of 1.40; these data are shown in Fig. 3.

Figure 6 presents data for K and K_2 at temperatures of 579 and 559 °K which imply an average molecular polarizability which is 1.42 and 1.37 greater than the atomic scalar polarizability, respectively.

Figure 7 shows representative data for Na and Na_2 at a temperature of 736 °K, and for Li and Li_2 at a temperature of 990 °K. For sodium, we obtained molecule/atom polarizability ratios of 1.27, 1.25, 1.29, and 1.26. For lithium, we measured molecule/atom polarizability ratios of 1.38, 1.36, and 1.41.

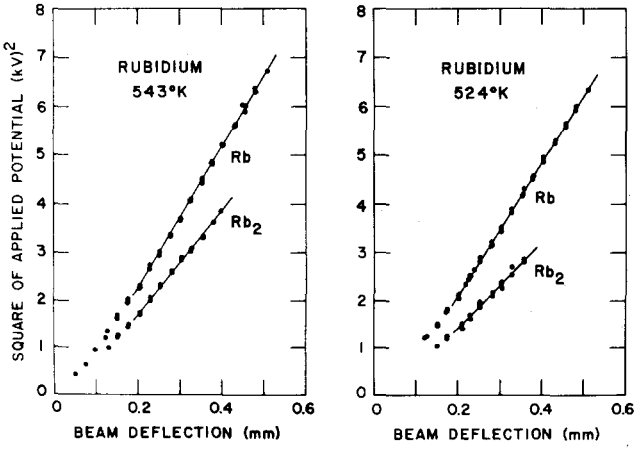

FIG. 5. Electric deflection results obtained for atomic and molecular rubidium beams. The slope of the deflection line is proportional to T/α.

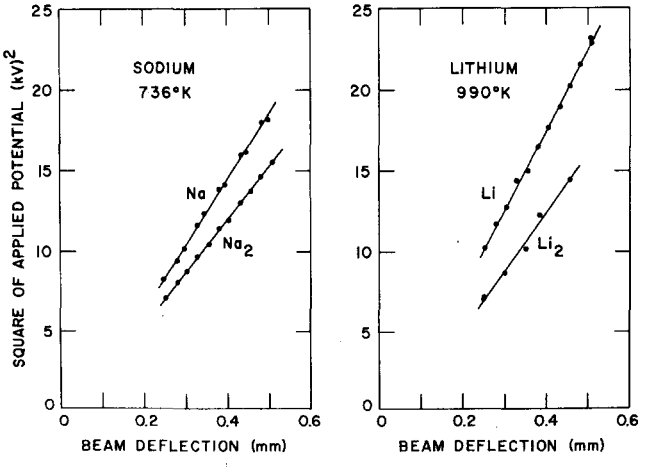

FIG. 7. Electric deflection results obtained for atomic and molecular sodium and lithium beams. The slope of the deflection line is porportional to T/α.

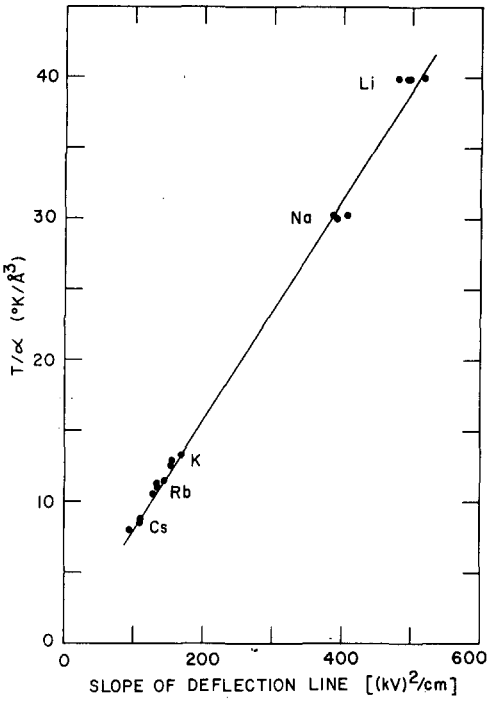

FIG. 8. A consistency test showing that the atomic deflection data yield relative atomic polarizabilities in agreement with accurate measurements of Ref. 5, which were used for the ordinate.

VI. ANALYSIS OF UNCERTAINTIES

A number of consistency tests have been made with this apparatus. Primarily, we have tested the correctness of the deflection analysis given in the Appendix. Figures 3–7 show that the data follow the expected behavior near the beam axis and at large deflections. In addition, one may compare the slopes of the V^2 vs Z lines at different temperatures for a given atomic species; the analysis in the Appendix predicts that the slope is directly proportional to the temperature and we indeed observe this. Similarly, we have verified that ratios of the slopes of the data we have presented in Figs. 3–7 for different atomic species agree with inverse ratios of the atomic polarizabilities of Ref. 5, correcting for the small temperature differences in each case. Our analysis yields the result that the data line slopes depend on T/α. For the atomic species α is known and we have plotted T/α vs the observed line slopes for all of our atomic data in Fig. 8. The consistency among the alkali atoms is seen to be good.

The work of Hall and Zorn[12] has shown that background gas scattering in a deflection experiment can introduce significant errors. It is partly for this reason that we chose to normalize the molecular results to the atomic polarizabilities rather than to trust absolute determinations. Even so, we must show that the energy distributions in the atomic and molecular beams are the same—that background gas scattering has not introduced any significant disparity. Our observation that the ratios of atomic data slopes agree with inverse polarizability ratios is already evidence that all of the particles have the same energy distributions at the same temperature, even the larger, slower species (e.g., Cs). We have made measurements of time-of-flight (TOF) distributions for the atomic and molecular beams, pulsing the beam mechanically and using the multichannel scaler to scan the arrival-time spectrum repetitively. In the analysis of the TOF data, it is necessary to include a parameter related to the time delay associated with the surface ionization process; this fact, coupled with the poor signal-to-noise ratio for the molecular data, limits the usefulness of the data. We have multiplied the time scale of the atomic TOF data by $\sqrt{2}$ and compared the spectra to the corresponding molecular spectra in each case. The results of the TOF analysis are self-consistent but cannot be said to be conclusive. Finally, we should point out that for the large deflections with which we deal, the particles that influence the maximum of the potential-scan spectra (Fig. 2) correspond to the high-velocity side of the velocity distribution.

We have made tests in which we deliberately offset the beam in the interaction region enough to cause a 5%–8% change in the slope of the V^2 vs Z data lines, but the polarizability ratio remains the same within our statistical uncertainty. This is characteristic of the normalization technique.

Although the geometrical constant describing the interaction region (the product CK^2 in the Appendix) does not enter the normalized polarizability determinations, we can measure this quantity from the atomic beam deflections using Eqs. (A10) and (A11) in the Appendix. We find $CK^2 = 847$ cm^{-1}. From E–H gradient balance data of Ref. 5, we can determine K^2 separately and obtain $C = 6.8$ cm^{-1} and $K = 11.16$ cm^{-1}.

The scatter in our data as shown in Figs. 3–7 is indicative of the statistical uncertainty in the experimental quantities V^2 and Z. We ascribe a 1% uncertainty to the relative V^2 measurements and a ± 0.0013 cm uncertainty in Z due to shifts in the undeflected beam position during data runs. The V^2 vs Z data slopes are accurate to about 3% within one standard deviation depending on the case at hand. In arriving at an over-all uncertainty of 8%–10% in the molecular polarizabilities (depending on the statistical uncertainty in each case), we include a 1% uncertainty in the ratio of the data line slopes, owing to the fact that they are distorted slightly by the finite beam width, and a 2% uncertainty in the values of the atomic polarizabilities.[5]

TABLE I. Our measured values of the average polarizabilities $\langle\bar{\alpha}\rangle_{J,v}$ of the alkali dimers at the temperatures given. The most probable rotational quantum number is J_m and the average vibrational quantum number is $\bar{v}$. The polarizabilities are given in units of 10^{-24} cm^3.

Species	T(°K)	$\langle\bar{\alpha}\rangle_{J,v}$	J_m	$\bar{v}$
Li_2	990	34 ± 3	22	1.5
Na_2	736	30 ± 3	40	2.7
K_2	569	61 ± 5	59	3.8
Rb_2	534	68 ± 7	88	6
Cs_2	515	91 ± 7	123	8

VII. CONCLUSIONS

An electric deflection technique has been used to measure the ratio of the average molecular polarizability to the atomic scalar polarizability for each of the alkali metal species. Since the atomic polarizabilities are known,[5] these measurements yield the average molecular polarizabilities listed in Table I at the temperatures given. The results are the best estimates resulting from more than one measurement in each case, some of which may correspond to slightly different temperatures which are assumed[10] to be equivalent. The measured polarizability is an average over the rotational and vibrational state distributions present in the beam at the temperatures indicated in Table I. We also list the most probable rotational quantum number J_m and the average vibrational quantum number $\bar{v}$ for the temperatures specified.

The only published calculation with which we may compare is that of Kolker and Karplus[1] for Li_2. They obtain an average polarizability of 52.29×10^{-24} cm^3. An unpublished calculation by Bottcher and Docken[7] gives values of 41.2×10^{-24} cm^3 for Li_2 and 36.7×10^{-24} cm^3 for Na_2. These calculated polarizabilities are considerably higher than our measured values of 34×10^{-24} cm^3 for Li_2 and 30×10^{-24} cm^3 for Na_2.

ACKNOWLEDGMENTS

The authors wish to thank Professor Howard H. Brown, Jr. for his advice throughout the course of this research and Professor Edward J. Robinson for a critical reading of the manuscript.

APPENDIX

The force exerted on a beam particle in the interaction region is $(\alpha_{zz}E)dE/dZ$. It is straightforward to show that the deflection Z of the particle at the detector is

$$Z=\kappa V^2\alpha_{zz}/mu^2\ , \tag{A1}$$

where m and u are the particle mass and speed, and $\kappa=CK^2L_1(L_1+2L_2)/2$. Here, C is the field gradient to field ratio characteristic of our pole pieces, K relates the field to the applied potential, L_1 is the length of the interaction region, and L_2 is the distance from the end of the interaction region to the detector.

Assuming an infinitesimal beam, our observed molecular beam intensity $I(Z, V)$ is proportional to the product of the velocity distribution and rotational state distribution, the former expressed in terms of the coordinate Z,

$$I(Z,V)dZ\sim\sum_J V^4\bar{\alpha}^2(2J+1)dZ \times\exp\{-\kappa V^2\bar{\alpha}/2ZkT)-[BhcJ(J+1)/kT]\}\ , \tag{A2}$$

where B is the rotational constant (in cm^{-1}), k is Boltzmann's constant, T is the source temperature, h is Planck's constant, c is the speed of light, and we have effected a sum over m_J by changing α_{zz} to $\bar{\alpha}$; for simplicity, we will not show the vibrational averaging. The maximum occurs for a potential V given by

$$\partial I/\partial V=0=\sum_J[2-(\kappa V^2\bar{\alpha}/2ZkT)]\bar{\alpha}^2(2J+1) \times\exp\{-(\kappa V^2\bar{\alpha}/2ZkT)-[BhcJ(J+1)/kT]\}\ . \tag{A3}$$

In order to solve this equation, we must assume a form for $\bar{\alpha}$. Consider

$$\bar{\alpha}=\alpha_0[1+qJ(J+1)]\ , \tag{A4}$$

which essentially states that the polarizability increases with internuclear distance; Eq. (A4) defines q. If we convert the sum in Eq. (A3) to an integral over J we make little error, since a great many J values are important (Table I). We find

$$0=\int_0^\infty[2-a(1+qx)](1+qx)^2dx\exp[-a(1+qx)-bx]\ , \tag{A5}$$

where $a=\kappa V^2\alpha_0/2ZkT$, $b=Bhc/kT$, and $x=J(J+1)$. The result of integration is

$$0=2-a+rq(4-3a)/b+2r^2q^2(2-3a)/b^2-6ar^3q^3/b^3\ , \tag{A6}$$

where $r=(1+aq/b)^{-1}$. An approximate solution to this equation is

$$a=2/(1+q/b) \tag{A7}$$

and is found to be accurate to within 1% for $q/b<0.3$.

The thermal average of the polarizability is $\langle\bar{\alpha}\rangle_J=\alpha_0(1+q/b)$. Combining this with Eq. (A7) we obtain

$$V^2=(4kT/\kappa\langle\bar{\alpha}\rangle_J)Z\ , \tag{A8}$$

which shows that the slope of the V^2 vs Z data line is inversely proportional to $\langle\bar{\alpha}\rangle_J$ for an infinitesimal beam and for $q/b<0.3$.

The parameter q/b indicates how the polarizability varies over the rotational states of interest. An estimate of q may be obtained[8] from the nonrigid rotator model[13] of the molecule:

$$q=(2B)^{3/2}h^{1/2}(\pi c\mu\omega)^{-1/2}\times10^8\ , \tag{A9}$$

where ω is the vibrational frequency parameter in cm^{-1}, μ is the atomic mass, and all quantities are in cgs units. Equations (A4) and (A9) agree with the results of a calculation by Kolos and Wolniewicz[14] for H_2. The change in the H_2 polarizability with vibrational quantum number also follows an expansion analogous to Eq. (A4). For the alkali dimers, we calculate typical q/b values of 0.06 which are so small that Eq. (A7) may be considered an exact solution to Eq. (A6).

For the alkali atoms, the polarizability is a scalar and one easily finds an equation similar to Eq. (A8),

$$V^2=(4kT/\kappa\alpha)Z\ , \tag{A10}$$

leading to the conclusion that the ratio of the molecular and atomic data lines slopes for infinitesimal beams gives the inverse ratio of the polarizabilities $\alpha/\langle\bar{\alpha}\rangle_{J,v}$.

If the finite size of the atom beam is taken into account, we obtain[8]

$$I(Z,V)\sim\int_0^\infty[F(Z_2)-F(Z_1)]e^{-y}dy\ , \tag{A11}$$

where $F(Z)$ is the beam profile along the detector line Z

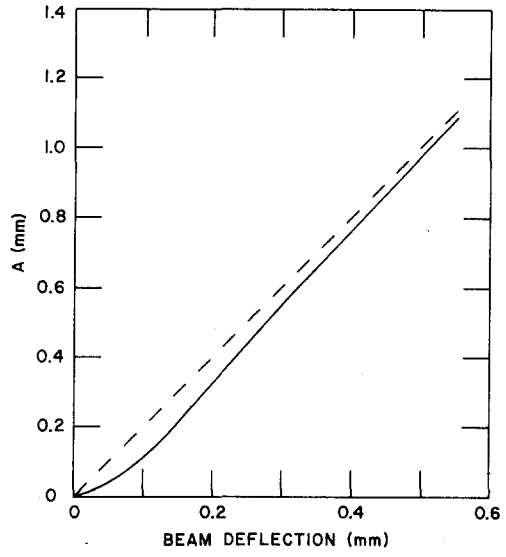

FIG. 9. A comparison of the deflection expected for an infinitesimal beam (dashed line) and for a finite beam (solid curve) using parameters given in Fig. 1. The quantitiy A is proportional to the square of the applied potential which gives the maximum beam intensity at the detector position, normalized with regard to temperature and polarizability to be the same for all atoms or molecules.

perpendicular to the beam axis, with $Z_{1,2} = Z - A/y \pm W$, where W is the detector half-width and $A = \kappa V^2 \alpha / 2kT$. A comparison of the expected results for an infinitesimal beam [Eq. (A10)] and a finite beam [Eq. (A11)] is given in Fig. 9, where the parameter $A \sim V^2$ is plotted vs the detector displacement Z.

The situation for a finite molecular beam is qualitatively the same as for a finite atomic beam. It is not necessary to go through the details of a finite-beam deflection analysis analogous to Eqs. (A1)–(A4) in order to see that the thermal average $\langle\bar{\alpha}\rangle_J$ is measured in the deflection experiment. The beam function $F(Z)$, where Z depends on $\bar{\alpha}$ and hence on J, is averaged over a thermal distribution function $g(J)$. Expanding F about α_0 [Eq. (A4)], we find

$$g(J)F(\bar{\alpha}) = F(\alpha_0) + \left(\frac{\partial F}{\partial \bar{\alpha}}\right)_{J=0} (\langle\bar{\alpha}\rangle_J - \alpha_0) + \frac{1}{2}\left(\frac{\partial^2 F}{\partial \bar{\alpha}^2}\right)_{J=0} (\langle\bar{\alpha}^2\rangle_J - 2\langle\bar{\alpha}\rangle_J \alpha_0 + \alpha_0^2) + \cdots \quad \text{(A12)}$$

$$= F(\langle\bar{\alpha}\rangle_J) - \frac{1}{2}\left(\frac{\partial^2 F}{\partial \bar{\alpha}^2}\right)_{J=0} (\langle\bar{\alpha}\rangle^2 - \langle\bar{\alpha}^2\rangle) \,. \quad \text{(A13)}$$

The second term in Eq. (A13) is the error term and is negligible if q/b is small. We have shown above [Eq. (A9) and following] that q/b is on the order of 0.06 for the alkali dimers. The vibrational averaging is similar.

In practice, we consider data from deflections of 0.015–0.051 cm in determining the slopes of the V^2 vs Z lines. In Fig. 9, it may be seen that the slope for the finite beam differs from the slope for the infinitesimal beam by 6%. In taking a ratio of the atomic and molecular slopes to obtain the inverse ratio of the polarizabilities, this difference cancels.

*Supported by the Army Research Office, Durham, and by the National Science Foundation. Details of much of the research reported here are contained in a thesis by R. W. M., submitted to the faculty of New York University in partial fulfillment of the requirements for the Ph. D. degree.

†Permanent address: Physics Department, University of Missouri at Rolla, Rolla, Missouri 65401.

[1] H. J. Kolker and M. Karplus, J. Chem. Phys. 39, 2011 (1963).
[2] W. Demtroder, M. McClintock, and R. N. Zare, J. Chem. Phys. 51, 5495 (1969).
[3] Y. T. Lee, R. J. Gordon, and D. R. Herschbach, J. Chem. Phys. 54, 2410 (1971), and W. S. Struve, T. Kitagawa, and D. R. Herschbach, J. Chem. Phys. 54, 2759 (1971).
[4] T. M. Miller and A. Kasdan, J. Chem. Phys. 59, 3913 (1973).
[5] R. W. Molof, H. L. Schwartz, T. M. Miller, and B. Bederson (to be published). The results are tabulated in Bull. Am. Phys. Soc. 18, 1500 (1973).
[6] B. Bederson and E. J. Robinson, Adv. Chem. Phys. 10, 1 (1966).
[7] C. Bottcher and K. Docken (private communication).
[8] R. W. Molof, Ph. D. thesis, New York University, 1974.
[9] K. B. MacAdam and N. F. Ramsey, Phys. Rev. A 6, 898 (1972).
[10] It is obvious that information about the rotational and vibrational state average could be deduced from measurements of $\langle\bar{\alpha}\rangle_{J,v}$ over a wide range of temperatures. However, in the Appendix we show that the changes in the polarizability with J and v are much too small to observe in this experiment. Although we do report here a few measurements at slightly different temperatures, the experiment is not precise enough to warrant drawing conclusions from the measured polarizability variations.
[11] A. Salop, E. Pollack, and B. Bederson, Phys. Rev. **124**, 1431 (1961).
[12] W. D. Hall and J. C. Zorn (unpublished). See Bull. Am. Phys. Soc. 12, 131 (1967).
[13] G. Herzberg, *Molecular Spectra and Molecular Structure I, Spectra of Diatomic Molecules* (Van Nostrand, Princeton, New Jersey, 1967).
[14] W. Kolos and L. Wolniewicz, J. Chem. Phys. **46**, 1426 (1967).